



Published in final edited form as:

*Oncogene*. 2015 January 15; 34(3): 394–402. doi:10.1038/onc.2013.577.

## ASC deficiency suppresses proliferation and prevents medulloblastoma incidence

Elizabeth R. W. Knight<sup>1,2</sup>, Esita Y. Patel<sup>2</sup>, Cornelius A. Flowers<sup>2</sup>, Andrew J. Crowther<sup>2,3</sup>, Jenny P. Ting<sup>1,3,4</sup>, C. Ryan Miller<sup>2,3,5,6</sup>, Timothy R. Gershon<sup>1,2,3,6</sup>, and Mohanish Deshmukh<sup>1,2,3,7</sup>

<sup>1</sup>Neurobiology Curriculum, UNC-Chapel Hill, Chapel Hill, NC 27599

<sup>2</sup>Neuroscience Center, UNC-Chapel Hill, Chapel Hill, NC 27599

<sup>3</sup>Lineberger Comprehensive Cancer Center, UNC-Chapel Hill, Chapel Hill, NC 27599

<sup>4</sup>Department of Microbiology & Immunology, UNC-Chapel Hill, Chapel Hill, NC 27599

<sup>5</sup>Department of Pathology and Laboratory Medicine, UNC-Chapel Hill, Chapel Hill, NC 27599

<sup>6</sup>Department of Neurology, UNC-Chapel Hill, Chapel Hill, NC 27599

<sup>7</sup>Department of Cell Biology & Physiology, UNC-Chapel Hill, Chapel Hill, NC 27599

### Abstract

Apoptosis-associated speck-like protein containing a caspase recruitment domain (ASC) is silenced by promoter methylation in many types of tumors, yet ASC's role in most cancers remains unknown. Here, we show that ASC is highly expressed in a model of medulloblastoma, the most common malignant pediatric brain cancer; ASC is also expressed in human medulloblastomas. Importantly, while ASC deficiency did not affect normal cerebellar development, ASC knock-out mice on the Smoothed (ND2:Sm $\alpha$ 1) transgenic model of medulloblastoma exhibited a profound reduction in medulloblastoma incidence and a delayed tumor onset. A similar decrease in tumorigenesis with ASC deficiency was also seen in the hGFAP-Cre:Sm $\alpha$ 2 mouse model of medulloblastoma. Interestingly, hyperproliferation of the external granule layer (EGL) was comparable at P20 in both the wildtype and ASC-deficient Sm $\alpha$ 1 mice. However, while the apoptosis and differentiation markers remained unchanged at this age, proliferation markers were decreased, and the EGL was reduced in thickness and area by P60. This reduction in proliferation with ASC deficiency was also seen in isolated Sm $\alpha$ 1 cerebellar granule precursor cells *in vitro*, indicating that the effect of ASC deletion on proliferation was cell autonomous. Interestingly, ASC deficient Sm $\alpha$ 1 cerebella exhibited disrupted expression of genes in the TGF- $\beta$  pathway and increased level of nuclear Smad3. Together, these results demonstrate an unexpected role for ASC in Sonic hedgehog-driven medulloblastoma tumorigenesis, thus identifying ASC as a promising novel target for anti-tumor therapy.

Correspondence should be addressed to: Mohanish Deshmukh, 7109E Neuroscience Research Building, 105 Mason Farm Road, University of North Carolina, Chapel Hill, NC 27599, Tel: (919) 843-6004, Fax: (919) 966-1050, mohanish@med.unc.edu.

### CONFLICT OF INTEREST

The authors declare no conflict of interest.

## Keywords

medulloblastoma; ASC; TMS-1; proliferation; TGF- $\beta$ ; tumor

---

## INTRODUCTION

Medulloblastoma, a tumor of cerebellar progenitors, is the most common malignant brain cancer in children<sup>1</sup>. During normal development, proliferation of progenitors in the cerebellum extends into the early postnatal period, as cerebellar granule neuron progenitors (CGNPs) undergo rapid division in the external granule layer (EGL), then differentiate and migrate to the internal granule layer (IGL)<sup>2</sup>. CGNPs proliferate in response to endogenous Sonic hedgehog (Shh; mouse), and mutations that activate SHH (human) signaling cause predisposition to medulloblastoma in humans with Gorlin Syndrome, and in genetically engineered mouse models<sup>1, 3</sup>. These models, which operate through either *Patched* deletion or insertion of constitutively active alleles of *Smoothened* (*Smo*), consistently implicate CGNPs as the cells of origin for Shh-driven medulloblastoma<sup>4, 5</sup>. Importantly, while advances in treatment have increased the survival of patients with medulloblastoma, mortality remains significantly high and debilitating cognitive and endocrine side effects result from current treatment regimens<sup>3</sup>. Thus, advancing the understanding of the genetic components of medulloblastoma tumorigenesis is needed to develop improved targeted therapies.

ASC (apoptosis-associated speck-like protein containing a caspase recruitment domain; also known as TMS-1, target of methylation-induced silencing-1 and Pycard) is expressed in many human tissues, however, is silenced by promoter hypermethylation in many tumor types, including glioblastoma<sup>6</sup>, neuroblastoma<sup>7</sup>, breast cancer<sup>8</sup>, melanoma<sup>9</sup>, and lung cancer<sup>10</sup>. Ectopic ASC expression sensitizes pancreatic, breast, and colon cancer cells to apoptosis<sup>8, 11–15</sup>, while knocking down endogenous ASC inhibits cell death of osteosarcoma cells<sup>13</sup>, colon cells<sup>15</sup>, and breast epithelial cells<sup>16</sup>. Additionally, ASC is the adaptor protein of the inflammasome, a cytosolic complex that senses pathogen-associated molecules and subsequently responds by activating pro-inflammatory substrates, pro-interleukin-1 $\beta$  (pro-IL-1 $\beta$ ) and pro-IL-18, which recruit and activate immune cells<sup>17–19</sup>. Consistent with the expectation that ASC inactivation promotes tumorigenesis, ASC-deficiency has been shown to enhance polyp formation in a colitis-associated colon cancer mouse model<sup>20, 21</sup>. Together, these studies point to ASC as a functional tumor suppressor.

In this study, we examined the role of ASC in medulloblastoma using mouse models. Our results reveal the unexpected finding that ASC promotes tumorigenesis in medulloblastoma. ASC was highly expressed in these tumors and the genetic deletion of ASC markedly reduced proliferation, hyperplasia, and mortality. These findings identify a novel role for ASC in promoting tumorigenesis in medulloblastoma.

## RESULTS AND DISCUSSION

### ASC is highly expressed in medulloblastomas

To investigate the role of ASC in cerebellar development and medulloblastoma, we evaluated ASC expression during mouse cerebellum development. ASC protein levels were high in postnatal-day 7 (P7) cerebellum, which corresponds to the peak period of CGNP cell proliferation, and decreased with cerebellar maturation (Figure 1a). ASC is reported to enhance apoptosis upon expression and is often silenced *via* methylation in a variety of cancers<sup>8, 11–14</sup>. To determine whether ASC was also silenced in cancer of cerebellar origin, we examined ASC expression in medulloblastoma. We used the ND2:SmoA1 (SmoA1) mouse model of medulloblastoma which expresses an activated allele of *Smo* in CGNPs, resulting in CGNP hyperproliferation and tumor growth as a consequence of the constitutive activation of the Sonic hedgehog pathway<sup>5</sup>. In contrast to the reports in other cancer types, we unexpectedly detected high levels of ASC in medulloblastoma (Figure 1a). Also, ASC mRNA levels closely matched protein levels throughout development and in the tumor (Figure 1b). These data reveal the surprising observation that ASC is not subjected to silencing but is induced in a mouse model of medulloblastoma.

To investigate ASC expression in human medulloblastomas, we conducted *in situ* hybridization (ISH) on sections of a tissue microarray (TMA) from 11 classic, 3 desmoplastic, and 1 large cell/anaplastic medulloblastomas obtained from 15 patients (8 males and 7 females; ages 1–38, median age=15). Overall, the majority (60%) were positive for ASC, including 45.5% of classic tumors, 100% of desmoplastic tumors, and the large cell/anaplastic tumor (Table 1). Classic tumors exhibited a range of ASC expression, while all desmoplastic tumors were positive for ASC expression (Figure 1c). Examination of publicly available gene expression profiling data in the Oncomine database also reveals ASC to be expressed in human medulloblastomas, with significantly increased expression in desmoplastic *versus* classic tumors (Figure 1d)<sup>22, 23</sup>. Furthermore, a recent paper reported ASC amplification to be a frequent genetic event in the human medulloblastomas studied<sup>24</sup>. Together, these data indicate that ASC is expressed in a significant portion of human medulloblastomas.

### ASC deficiency does not affect normal cerebellum development

To investigate whether ASC expression is important in medulloblastoma tumorigenesis, we first evaluated whether ASC deficiency affected normal cerebellar development. Cerebellar development occurs postnatally with rapid CGNP proliferation in the EGL peaking at P7. As CGNPs terminally differentiate into cerebellar granule neurons (CGNs), they migrate to the IGL to form the mature cerebellum by P20<sup>2</sup>. We therefore compared cerebellar architecture of ASC<sup>+/+</sup> and ASC<sup>-/-</sup> mice during this key developmental period. H&E staining revealed no differences in gross morphology between wild-type and ASC-deficient cerebella throughout development (Figure 1e). To specifically examine whether proliferation was altered by ASC deficiency, we compared expression of proliferation markers cyclin D2 and phospho-histone H3 (pH3) in ASC<sup>+/+</sup> and ASC<sup>-/-</sup> P7 cerebellum. No differences in cyclin D2 levels and pH3 staining were observed between wild-type and ASC-deficient cerebella (Figures 1f and g).

### ASC deficiency suppresses SmoA1- and SmoM2-induced medulloblastoma

Next, to determine whether ASC deficiency affects medulloblastoma, we generated ASC<sup>+/+</sup>, ASC<sup>+/-</sup>, and ASC<sup>-/-</sup> SmoA1 mice and compared the time of tumor emergence in each group. In this Smo transgenic medulloblastoma model, signs of tumors typically emerge at 3–8 months and precede death from the disease by only a few days; thus, once signs emerge, mice are in a moribund state<sup>5</sup>. Surprisingly, ASC deficiency conferred a striking reduction in tumor incidence and delay in tumor onset in the transgenic mice (Figure 2a). Overall tumor incidence by P300 was significantly reduced in mice lacking ASC: while 12 of 15 ASC<sup>+/+</sup>;SmoA1 mice exhibited tumors, only 5 of 18 ASC<sup>-/-</sup>;SmoA1 mice developed medulloblastoma (Figure 2b). Additionally, ASC deficiency markedly delayed latency to tumor formation in ASC<sup>-/-</sup>;SmoA1 mice compared to ASC<sup>+/+</sup>;SmoA1 and ASC<sup>+/-</sup>;SmoA1 mice (Figure 2a). ASC heterozygous mice also exhibited a delayed rate of tumorigenesis when compared to wild-type mice (Figure 2a).

To test whether ASC deficiency affects tumorigenesis in another model of medulloblastoma, we utilized the SmoM2 model. SmoM2 is a constitutively active Shh-driving *Smo* mutation discovered to aggressively induce medulloblastoma in mice by P20<sup>25–27</sup>. We generated ASC<sup>+/+</sup>, ASC<sup>+/-</sup>, and ASC<sup>-/-</sup> hGFAP-Cre:SmoM2 (SmoM2) mice and evaluated time to tumor emergence and moribund status. ASC deficiency markedly reduced tumorigenesis in the SmoM2 model, with loss of even one ASC allele extending survival (Figure 2c). While all mice developed medulloblastoma in this model, the average age at which mice became moribund was delayed in ASC heterozygous and knock-out mice (Figure 2d). Thus, ASC deficiency profoundly reduced tumorigenesis and extended survival in two distinct mouse models of medulloblastoma.

One of the known functions of ASC is that it is an adaptor protein for the inflammasome, a complex that, when triggered by intracellular signals, cleaves proinflammatory substrate pro-IL-1 $\beta$  into its active form<sup>17–19</sup>. IL-1 $\beta$  has been reported to have several functions promoting cancer<sup>28</sup>, although it has not been studied in medulloblastoma. To determine whether IL-1 $\beta$  is required for medulloblastoma development, we evaluated tumorigenesis in IL-1 $\beta$  deficient mice in the SmoA1 model. In contrast to our results with the loss of ASC, IL-1 $\beta$  deficiency did not affect medulloblastoma onset or incidence (Supplemental Figure 1).

To determine the point at which ASC deficiency blocks tumorigenesis in medulloblastoma, we compared wild-type and ASC-deficient SmoA1 cerebella at multiple time points during tumor development. In this tumor model, ectopic CGNP proliferation can be detected by P20 and progresses into tumor in adulthood. To examine whether ASC deficiency affects CGNP hyperproliferation during the pre-tumor stages (P20, P60), histological H&E stained sections of ASC<sup>+/+</sup> and ASC<sup>-/-</sup> SmoA1 cerebella were compared. ASC<sup>-/-</sup>;SmoA1 cerebella exhibited equivalent ectopic CGNP proliferation and EGL architecture as seen in ASC<sup>+/+</sup>;SmoA1 mice at P7 and P20. However, by P60, ASC deletion significantly reduced the proportion and thickness of EGL in the cerebella (Figures 3a, b, and c). Thus, ASC deficiency did not block the initial stages of CGNP hyperproliferation but markedly diminished ectopic EGL in the cerebellum by P60.

### ASC deficient SmoA1 cerebella exhibit reduced proliferation

Tumorigenesis can be regulated by the balance of proliferation, differentiation, and apoptosis. We sought to determine which factors were responsible for the requirement of ASC in Shh-driven medulloblastoma. To test whether proliferation was altered in the ASC knock-out cerebella in the SmoA1 medulloblastoma model, we performed Western blot analysis for cyclin D2 and immunohistochemistry for the mitotic marker pH3 in wild-type and ASC-deficient SmoA1 mice. Cyclin D2 levels were unchanged at P7, but were strikingly reduced by P60, at which point cyclin D2 levels were virtually undetectable in the ASC-deficient mice but were sustained in the wild-type mice on the SmoA1 background (Figure 3d). Thus, even though gross reduction in hyperplasia was not detected by P20 in the ASC<sup>-/-</sup>;SmoA1 cerebella, markers of proliferation showed an emerging trend of reduction at this time point. To directly test whether ASC expression affected proliferation of the CGNPs in the EGL, we conducted pH3 immunohistochemistry. Consistent with the reduction in cyclin D2 levels, pH3 staining was reduced by nearly 50 % at P20, revealing a lower mitotic frequency in the EGL with ASC deletion (Figures 3e and f). These results identify a role for ASC in regulating ectopic proliferation of CGNPs in medulloblastoma *in vivo*.

We next examined whether the effect of ASC on proliferation of CGNPs in this tumor model was cell autonomous. CGNPs from ASC<sup>+/-</sup>;SmoA1 and ASC<sup>-/-</sup>;SmoA1 mice were isolated and maintained for two days *in vitro*. Western blot analysis revealed that ASC deficiency reduced the proliferation marker cyclin D2 even in these isolated tumor cells (Figure 3g). These data suggest a cell intrinsic effect of ASC on CGNP proliferation in the SmoA1 model. However, we cannot exclude the possibility that ASC deficiency could also affect stromal signals to modulate CGNP proliferation *in vivo*.

Previous studies have reported a decrease in proliferation with ASC deficiency in stimulated CD4<sup>+</sup> and CD8<sup>+</sup> T cells, splenocytes, and lymph node cells<sup>29-31</sup>. However, other studies have reported either no difference in proliferation of ASC knock-out splenocytes or an increase in proliferation with ASC deletion in keratinocytes<sup>32, 33</sup>. Together, these data point to a complex role for ASC in regulating cell proliferation, with our results showing that ASC deficiency markedly reduces proliferation in medulloblastoma.

Numerous studies have shown that ASC is proapoptotic when overexpressed in cancer cell lines<sup>8, 11-15</sup>. Furthermore, knockdown of endogenous ASC reduces apoptosis of breast epithelial cells<sup>16</sup>, colon cancer cells<sup>15</sup>, and osteosarcoma cells<sup>13</sup>. We examined whether ASC altered apoptosis or differentiation during tumorigenesis and found no statistical differences in the differentiation marker NeuN or the apoptosis marker cleaved caspase-3 between wild-type and ASC-deficient P20 SmoA1 EGL (Figures 3e and f). Likewise, other groups have found no difference in apoptosis with loss of endogenous ASC in keratinocytes or splenocytes<sup>31, 33</sup>. Together, these results identify reduced proliferation as the likely key factor suppressing medulloblastoma tumorigenesis in ASC deficient mice.

### ASC deficient SmoA1 cerebella exhibit altered TGF- $\beta$ pathway gene expression and increased nuclear Smad3

To determine the mechanism by which ASC deficiency inhibits proliferation in medulloblastoma, we conducted a microarray analysis comparing gene expression of ASC<sup>-/-</sup> versus ASC<sup>+/+</sup> cerebella on the SmoA1 background. We focused on P20 because the differences in the ASC<sup>-/-</sup> and ASC<sup>+/+</sup> cerebellar phenotypes begin to emerge at this timepoint. Microarray data are available in Gene Expression Omnibus under the accession number GSE48682. Microarray analysis revealed only 3 genes (in addition to ASC) to be differentially expressed between ASC<sup>-/-</sup> and ASC<sup>+/+</sup> SmoA1 cerebellum at this timepoint (Table 2). The fact that only a small number of genes were identified to be differentially expressed is not surprising as differences in the tumor phenotype are just emerging at the P20 timepoint. Of the 3 differentially-expressed genes identified, *Tgfb1l1* (transforming growth factor beta-1-induced transcript 1), which was 2.5 fold higher in the ASC knock-out samples, is known to be upregulated with TGF- $\beta$  (transforming growth factor- $\beta$ )<sup>34</sup>. Interestingly, *Tgfb1l1* (also known as *Hic-5*) has been reported to inhibit cell proliferation when overexpressed in cells<sup>35, 36</sup>. We next examined whether the TGF- $\beta$  pathway was altered in the absence of ASC. Indeed, quantitative PCR analysis confirmed dysregulation of TGF- $\beta$  pathway genes in the knock-out, with *Tgfb1l1* significantly upregulated while the TGF- $\beta$  inhibitor *Tgif1* was significantly downregulated in ASC-deficient P20 SmoA1 mice. Furthermore, cell cycle genes *cyclin D2* and *Cdk2* were decreased in the ASC knock-out SmoA1 cerebella (Figure 4a).

Dysregulation of the TGF- $\beta$  pathway has been recognized in a subgroup of medulloblastomas<sup>37-39</sup>. To investigate whether TGF- $\beta$  signaling is altered in ASC<sup>-/-</sup> transgenic cerebella, we evaluated cellular phospho-Smad3 localization using immunohistochemistry. Interestingly, we found a greater percentage of cells with nuclear Smad3 in the ASC deficient transgenic cerebella (Figure 4b). These data reveal an unexpected link between ASC and the TGF- $\beta$  pathway whereby ASC deficient cerebella exhibit altered TGF- $\beta$  pathway gene expression and increased nuclear Smad3 in a mouse model of medulloblastoma.

Interestingly, TGF- $\beta$  activation has a dual role in cancer, as the pathway promotes epithelial-mesenchymal transition and metastasis, but early TGF- $\beta$  activation restricts tumorigenesis by inducing apoptosis and reducing cell proliferation<sup>40, 41</sup>. The dichotomous effects of the TGF- $\beta$  pathway are evident in medulloblastoma. One group found disruption of TGF- $\beta$  pathway genes in one of four subsets of medulloblastoma, namely deletion of TGF- $\beta$  inhibitors and amplification of Type II activin receptors and *TGFBR1*<sup>37</sup>. In contrast, we observed an association between increased TGF- $\beta$  pathway gene expression and signaling and decreased CGNP proliferation in the ASC knock-out SmoA1 P20 cerebella. Consistent with our results, increasing TGF- $\beta$  signaling with BMP2/4 addition or Smad5 overexpression in the presence of Shh stimulation reduces CGNP proliferation<sup>42, 43</sup>. Furthermore, increased nuclear Smad3 in SHH-related human medulloblastomas is correlated with a more favorable prognosis<sup>38</sup>.

While these results in medulloblastoma identify a clear role of ASC in promoting tumorigenesis, ASC has also been described as a tumor suppressor in specific cancer models. ASC suppresses tumorigenesis in a colitis-associated colon cancer mouse model, where ASC deficiency enhanced polyp formation and clinical exacerbation, resulting in reduced survival<sup>20, 21</sup>. In a model of squamous cell carcinoma, selective deletion of ASC in bone marrow derived macrophages suppressed tumor number but ASC ablation in keratinocytes promoted tumorigenesis<sup>33</sup>. When ASC was deleted from the whole animal, ASC knock-out mice showed no differences from wild-type in tumor susceptibility<sup>33</sup>. In melanoma, a recent study found that ASC-deficient metastatic melanoma cells injected into nude mice displayed reduced tumor growth as compared to wild-type tumor cell implantation. In contrast, ASC-deficient primary melanoma implants hastened tumor growth versus wild-type controls<sup>44</sup>. Thus, the role of ASC in carcinogenesis appears to depend on the cancer, cell type, and stage of cancer progression.

In summary, our results identify a critical function of ASC in driving proliferation and tumorigenesis in Shh pathway-driven models of medulloblastoma. Improved therapeutics for this cancer are needed due to the high mortality and devastating side effects of current treatment. Our results show that targeting ASC may be a promising strategy for preventing tumor progression of medulloblastoma.

## Supplementary Material

Refer to Web version on PubMed Central for supplementary material.

## Acknowledgments

We thank Drs. Vishva Dixit (Genentech), James Olson (Fred Hutchinson Cancer Research Center), Eva Anton (UNC) for generously sharing ASC<sup>-/-</sup>, ND2;SmoA1, and hGFAP-cre mice, respectively. We appreciate the technical assistance provided by Vivian Xu, Michael Conlin, and Meera Patel in the Deshmukh Lab; Janice Weaver, Lily Wai, and Yongjuan Xia in the UNC Histopathology Core; Terese Camp and Ling Li in the UNC Genomics Core; Mark Vincent Olorvida, Stephanie Cohen, and Bentley Midkiff in the UNC Translational Pathology Laboratory (TPL); and Joel Parker, George Wu, Chandri Yandava, and Chris Fan at UNC for bioinformatics and biostatistics guidance. The UNC TPL is supported in part by grants from the National Cancer Institute (3P30CA016086) and the UNC University Cancer Research Fund. We would like to thank members of the Deshmukh laboratory for critical review of this manuscript. TRG is supported by NIH grant 1K08NS077978 and St. Baldrick's Foundation. This work was supported by grants NS042197 and GM078366 to MD.

## References

1. Hatten M, Roussel M. Development and cancer of the cerebellum. *Trends Neurosci.* 2011; 34:134–142.
2. Hatten ME, Heintz N. Mechanisms of neural patterning and specification in the developing cerebellum. *Annu Rev Neurosci.* 1995; 18:385–408. [PubMed: 7605067]
3. Polkinghorn WR, Tarbell NJ. Medulloblastoma: tumorigenesis, current clinical paradigm, and efforts to improve risk stratification. *Nat Clin Pract Oncol.* 2007; 4:295–304. [PubMed: 17464337]
4. Yang ZJ, Ellis T, Markant SL, Read TA, Kessler JD, Bourbonoulas M, et al. Medulloblastoma can be initiated by deletion of Patched in lineage-restricted progenitors or stem cells. *Cancer Cell.* 2008; 14:135–145. [PubMed: 18691548]
5. Hallahan AR, Pritchard JI, Hansen S, Benson M, Stoeck J, Hatton BA, et al. The SmoA1 mouse model reveals that notch signaling is critical for the growth and survival of sonic hedgehog-induced medulloblastomas. *Cancer Res.* 2004; 64:7794–7800. [PubMed: 15520185]

6. Stone AR, Bobo W, Brat DJ, Devi NS, Van Meir EG, Vertino PM. Aberrant methylation and down-regulation of TMS1/ASC in human glioblastoma. *Am J Pathol.* 2004; 165:1151–1161. [PubMed: 15466382]
7. Alaminos M, Davalos V, Cheung NK, Gerald WL, Esteller M. Clustering of gene hypermethylation associated with clinical risk groups in neuroblastoma. *J Natl Cancer Inst.* 2004; 96:1208–1219. [PubMed: 15316056]
8. Conway KE, McConnell BB, Bowring CE, Donald CD, Warren ST, Vertino PM. TMS1, a novel proapoptotic caspase recruitment domain protein, is a target of methylation-induced gene silencing in human breast cancers. *Cancer Res.* 2000; 60:6236–6242. [PubMed: 11103776]
9. Guan X, Sagara J, Yokoyama T, Koganehira Y, Oguchi M, Saida T, et al. ASC/TMS1, a caspase-1 activating adaptor, is downregulated by aberrant methylation in human melanoma. *Int J Cancer.* 2003; 107:202–208. [PubMed: 12949795]
10. Machida EO, Brock MV, Hooker CM, Nakayama J, Ishida A, Amano J, et al. Hypermethylation of ASC/TMS1 is a sputum marker for late-stage lung cancer. *Cancer Res.* 2006; 66:6210–6218. [PubMed: 16778195]
11. Ramachandran K, Miller H, Gordian E, Rocha-Lima C, Singal R. Methylation-mediated silencing of TMS1 in pancreatic cancer and its potential contribution to chemosensitivity. *Anticancer Res.* 2010; 30:3919–3925. [PubMed: 21036703]
12. Parsons MJ, Vertino PM. Dual role of TMS1/ASC in death receptor signaling. *Oncogene.* 2006; 25:6948–6958. [PubMed: 16715133]
13. Ohtsuka T, Ryu H, Minamishima YA, Macip S, Sagara J, Nakayama KI, et al. ASC is a Bax adaptor and regulates the p53-Bax mitochondrial apoptosis pathway. *Nat Cell Biol.* 2004; 6:121–128. [PubMed: 14730312]
14. Ohtsuka T, Liu XF, Koga Y, Kitajima Y, Nakafusa Y, Ha CW, et al. Methylation-induced silencing of ASC and the effect of expressed ASC on p53-mediated chemosensitivity in colorectal cancer. *Oncogene.* 2006; 25:1807–1811. [PubMed: 16331272]
15. Hong S, Hwang I, Lee YS, Park S, Lee WK, Fernandes-Alnemri T, et al. Restoration of ASC expression sensitizes colorectal cancer cells to genotoxic stress-induced caspase-independent cell death. *Cancer Lett.* 2013; 331:183–191. [PubMed: 23321501]
16. Parsons MJ, Patel P, Brat DJ, Colbert L, Vertino PM. Silencing of TMS1/ASC promotes resistance to anoikis in breast epithelial cells. *Cancer Res.* 2009; 69:1706–1711. [PubMed: 19223547]
17. Fernandes-Alnemri T, Yu JW, Datta P, Wu J, Alnemri ES. AIM2 activates the inflammasome and cell death in response to cytoplasmic DNA. *Nature.* 2009; 458:509–513. [PubMed: 19158676]
18. Franchi L, Eigenbrod T, Munoz-Planillo R, Nunez G. The inflammasome: a caspase-1-activation platform that regulates immune responses and disease pathogenesis. *Nature Immunol.* 2009; 10:241–247. [PubMed: 19221555]
19. Davis BK, Wen H, Ting JP. The inflammasome NLRs in immunity, inflammation, and associated diseases. *Annu Rev Immunol.* 2011; 29:707–735. [PubMed: 21219188]
20. Allen IC, TeKippe EM, Woodford R-MT, Uronis JM, Holl EK, Rogers AB, et al. The NLRP3 inflammasome functions as a negative regulator of tumorigenesis during colitis-associated cancer. *J Exp Med.* 2010; 207:1045–1056. [PubMed: 20385749]
21. Zaki MH, Vogel P, Body-Malapel M, Lamkanfi M, Kanneganti T-D. IL-18 production downstream of the Nlrp3 inflammasome confers protection against colorectal tumor formation. *J Immunol.* 2010; 185:4912–4920. [PubMed: 20855874]
22. Kool M, Koster J, Bunt J, Hasselt NE, Lakeman A, van Sluis P, et al. Integrated genomics identifies five medulloblastoma subtypes with distinct genetic profiles, pathway signatures and clinicopathological features. *PLoS One.* 2008; 3:e3088. [PubMed: 18769486]
23. Fattet S, Haberler C, Legoux P, Varlet P, Lellouch-Tubiana A, Lair S, et al. Beta-catenin status in paediatric medulloblastomas: correlation of immunohistochemical expression with mutational status, genetic profiles, and clinical characteristics. *J Pathol.* 2009; 218:86–94. [PubMed: 19197950]
24. Feierabend D, Walter J, Grube S, Herbold C, Beetz C, Kalff R, et al. Methylation-specific multiplex ligation-dependent probe amplification and its impact on clinical findings in medulloblastoma. *J Neurooncol.* 2013; 107/s11060-11013-11286-11060



25. Xie J, Murone M, Luoh S-M, Ryan A, Gu Q, Zhang C, et al. Activating Smoothed mutations in sporadic basal-cell carcinoma. *Nature*. 1998; 391:90–92. [PubMed: 9422511]
26. Mao J, Ligon KL, Rakhlin EY, Thayer SP, Bronson RT, Rowitch D, et al. A Novel Somatic Mouse Model to Survey Tumorigenic Potential Applied to the Hedgehog Pathway. *Cancer Res*. 2006; 66:10171–10178. [PubMed: 17047082]
27. Jeong J, Mao J, Tenzen T, Kottmann AH, McMahon AP. Hedgehog signaling in the neural crest cells regulates the patterning and growth of facial primordia. *Genes Dev*. 2004; 18:937–951. [PubMed: 15107405]
28. Apte R, Dotan S, Elkabets M, White M, Reich E, Carmi Y, et al. The involvement of IL-1 in tumorigenesis, tumor invasiveness, metastasis and tumor-host interactions. *Cancer Metastasis Rev*. 2006; 25:387–408. [PubMed: 17043764]
29. Narayan S, Kolly L, So A, Busso N. Increased interleukin-10 production by ASC-deficient CD4+ T cells impairs bystander T-cell proliferation. *Immunology*. 2011; 134:33–40. [PubMed: 21718313]
30. Ippagunta SK, Brand DD, Luo J, Boyd KL, Calabrese C, Stienstra R, et al. Inflammasome-independent role of apoptosis-associated speck-like protein containing a CARD (ASC) in T cell priming is critical for collagen-induced arthritis. *J Biol Chem*. 2010; 285:12454–12462. [PubMed: 20177071]
31. Kolly L, Karababa M, Joosten LA, Narayan S, Salvi R, Petrilli V, et al. Inflammatory role of ASC in antigen-induced arthritis is independent of caspase-1, NALP-3, and IPAF. *J Immunol*. 2009; 183:4003–4012. [PubMed: 19717512]
32. Shaw PJ, Lukens JR, Burns S, Chi H, McGargill MA, Kanneganti TD. Cutting edge: critical role for PYCARD/ASC in the development of experimental autoimmune encephalomyelitis. *J Immunol*. 2010; 184:4610–4614. [PubMed: 20368281]
33. Drexler SK, Bonsignore L, Masin M, Tardivel A, Jackstadt R, Hermeking H, et al. Tissue-specific opposing functions of the inflammasome adaptor ASC in the regulation of epithelial skin carcinogenesis. *Proc Natl Acad Sci U S A*. 2012; 109:18384–18389. [PubMed: 23090995]
34. Shibamura M, Mashimo J, Mita A, Kuroki T, Nose K. Cloning from a mouse osteoblastic cell line of a set of transforming-growth-factor-beta 1-regulated genes, one of which seems to encode a follistatin-related polypeptide. *Eur J Biochem*. 1993; 217:13–19. [PubMed: 7901004]
35. Shibamura M, Nose K. Forced expression of hic-5, a senescence-related gene, potentiates a differentiation process of RCT-1 cells induced by retinoic acid. *Int J Biochem Cell Biol*. 1998; 30:39–45. [PubMed: 9597752]
36. Dabiri G, Tumbarello DA, Turner CE, Van de Water L. TGF-beta1 slows the growth of pathogenic myofibroblasts through a mechanism requiring the focal adhesion protein, Hic-5. *J Invest Dermatol*. 2008; 128:280–291. [PubMed: 17671518]
37. Northcott PA, Shih DJ, Peacock J, Garzia L, Morrissy AS, Zichner T, et al. Subgroup-specific structural variation across 1,000 medulloblastoma genomes. *Nature*. 2012; 488:49–56. [PubMed: 22832581]
38. Aref D, Moffatt CJ, Agnihotri S, Ramaswamy V, Dubuc AM, Northcott PA, et al. Canonical TGF-beta Pathway Activity Is a Predictor of SHH-Driven Medulloblastoma Survival and Delineates Putative Precursors in Cerebellar Development. *Brain Pathol*. 2012; 23:178–191. [PubMed: 22966790]
39. Cho YJ, Tsherniak A, Tamayo P, Santagata S, Ligon A, Greulich H, et al. Integrative genomic analysis of medulloblastoma identifies a molecular subgroup that drives poor clinical outcome. *J Clin Oncol*. 2011; 29:1424–1430. [PubMed: 21098324]
40. Massague J. TGFbeta in Cancer. *Cell*. 2008; 134:215–230. [PubMed: 18662538]
41. Rich JN. The role of transforming growth factor-beta in primary brain tumors. *Front Biosci*. 2003; 8:e245–260. [PubMed: 12456378]
42. Rios I, Alvarez-Rodriguez R, Marti E, Pons S. Bmp2 antagonizes sonic hedgehog-mediated proliferation of cerebellar granule neurones through Smad5 signalling. *Development*. 2004; 131:3159–3168. [PubMed: 15197161]

43. Zhao H, Ayrault O, Zindy F, Kim J-H, Roussel MF. Post-transcriptional down-regulation of Atoh1/Math1 by bone morphogenic proteins suppresses medulloblastoma development. *Genes Dev.* 2008; 22:722–727. [PubMed: 18347090]
44. Liu W, Luo Y, Dunn JH, Norris DA, Dinarello CA, Fujita M. Dual Role of Apoptosis-Associated Speck-Like Protein Containing a CARD (ASC) in Tumorigenesis of Human Melanoma. *J Invest Dermatol.* 2013; 133:518–527. [PubMed: 22931929]
45. Kole AJ, Swahari V, Hammond SM, Deshmukh M. miR-29b is activated during neuronal maturation and targets BH3-only genes to restrict apoptosis. *Genes Dev.* 2011; 25:125–130. [PubMed: 21245165]
46. Kenney AM, Cole MD, Rowitch DH. Nmyc upregulation by sonic hedgehog signaling promotes proliferation in developing cerebellar granule neuron precursors. *Development.* 2003; 130:15–28. [PubMed: 12441288]

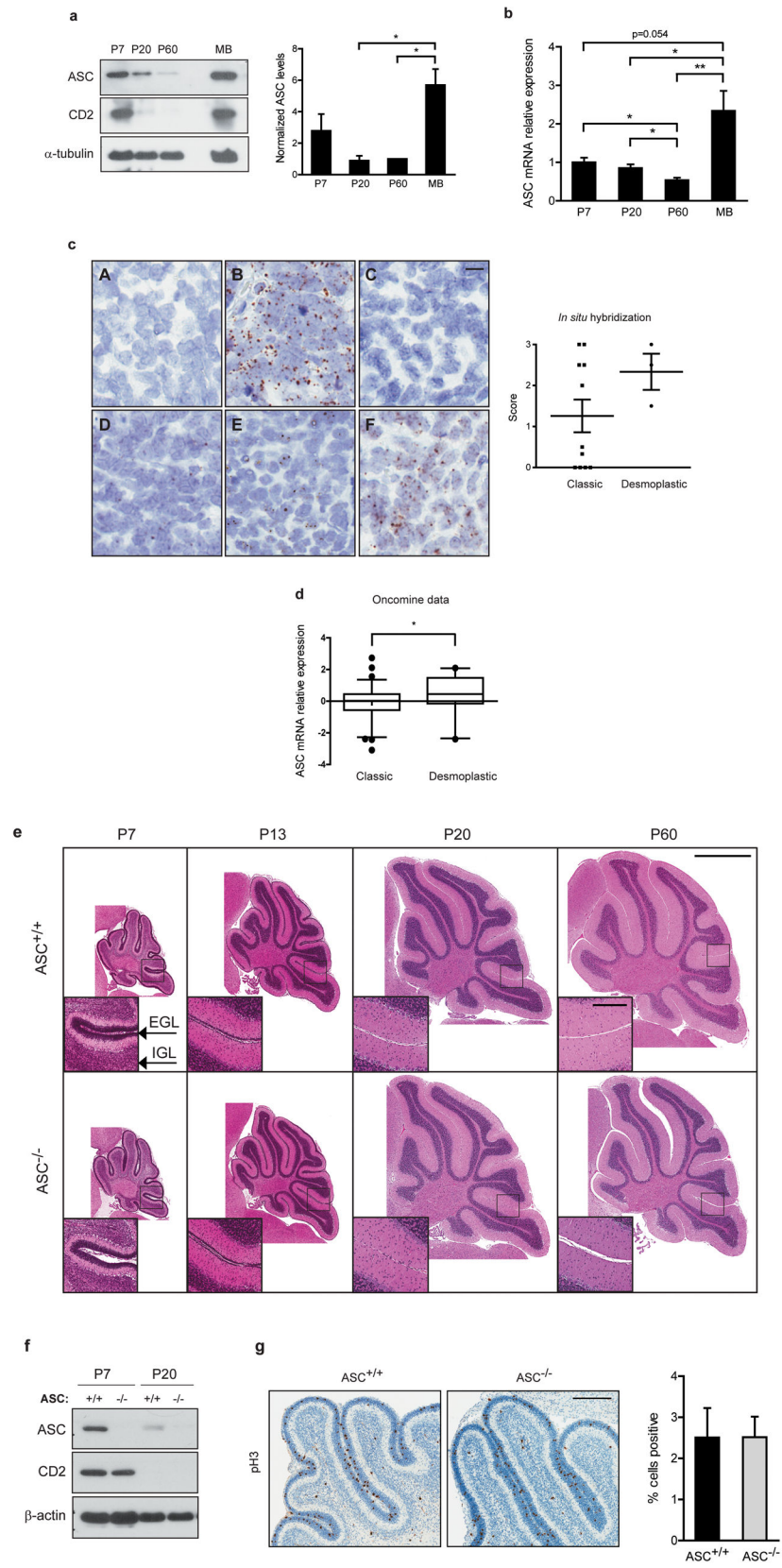


**Figure 1.**

ASC is expressed in cerebellum and medulloblastoma but ASC deficiency does not affect normal cerebellum development. **(a)** Western blot analysis of cerebellar lysates reveals ASC expression during normal cerebellum development and increased ASC expression in medulloblastoma. (Tumor sample shown is from postnatal 101-day-old, P101, mouse.) Densitometric quantification reveals ASC levels are increased in medulloblastomas. Data are mean of four separate experiments  $\pm$  s.e.m. analyzed by Student's *t*-test ( $P=0.014$ ,  $0.019$ ) and one-way ANOVA ( $P=0.029$ );  $n=3-4$  per group. ASC levels are normalized to loading controls and average P60 levels were set to 1.0 for each experiment.  $*P<0.05$ . Cerebella were collected at specified ages and lysates were probed with antibodies against ASC (Alexis Biochemicals, Lausen, Switzerland; Adipogen, San Diego, CA, USA), Cyclin D2 (CD2; Cell Signaling, Danvers, MA, USA) and  $\alpha$ -tubulin (Sigma-Aldrich, St. Louis, MO, USA). **(b)** Quantitative RT-PCR analysis demonstrates ASC mRNA decreases during normal cerebellum development and is induced in medulloblastoma. Cerebella were collected at the ages specified ( $n=4-6$  per age). Tumors were collected at an average age of P138 (P101-P205;  $n=8$ ). qRT-PCR was conducted similarly as previously described<sup>45</sup>, using primers *Pycard*-FW: 5'-GACCAGCACAGGCAAGCA-3', *Pycard*-Rev: 5'-TCCAGCACTCCGTCCTTC-3', *Gapdh*-FW: 5'-TGTGTCGTCGTTGGATCTGA-3', and *Gapdh*-Rev: 5'-CCTGCTTACCACCTTCTTGA-3', and normalizing to GAPDH levels. Data are mean  $\pm$  s.e.m analyzed by the Mann-Whitney test. Experiments were done in triplicate four times.  $**P<0.01$ ;  $*P<0.05$ . **(c)** RNA *in situ* hybridization (ISH) of human medulloblastoma tissue microarray sections for **(A)** DapB (negative control), **(B)** PPIB (positive control), and four representative samples where ASC expression was scored as **(C)** 0 (no signal), **(D)** 1 (rare signal), **(E)** 2 (scattered signal) or **(F)** 3 (ubiquitous signal). RNA ISH was performed and ASC expression was quantified as described in Table 1. The scatter plot shows mean ASC expression score and s.e.m. for classic and desmoplastic tumors. The average score was 1.3 for classic tumors ( $n=11$ ), 2.3 for desmoplastic tumors ( $n=3$ ), and 2.0 for large cell/anaplastic medulloblastoma ( $n=1$ ). The difference between the desmoplastic and classic groups was not significant ( $P=0.12$ ; Student's *t*-test). No correlation between ASC score and age or gender was observed. Scale bar represents 10  $\mu$ m. **(d)** OncoPrint analysis of independent gene profiling studies, with data from Kool *et al.*<sup>22</sup> and Fattet *et al.*<sup>23</sup> was used to compare ASC mRNA expression levels in classic versus desmoplastic human primary medulloblastomas. Each dataset had equivalent proportions of desmoplastic tumors (22%) and classic tumors (78%) and F-test analysis determined the datasets did not have unequal variance ( $F=0.054$ ). Data are medians with 95% confidence intervals for ASC mRNA in the combined datasets ( $*P=0.047$ , two-tailed *t*-test;  $n=74$  classic;  $n=21$  desmoplastic). Correction for potential technical bias between datasets, by adjusting values to make each dataset mean equal zero, yielded similar results ( $P=0.025$ ; data not shown). **(e)** Representative images of H&E stained sagittal sections of ASC<sup>+/+</sup> and ASC<sup>-/-</sup> cerebella at specified ages show no differences in gross cerebellar architecture with development between genotypes ( $n=3-8$  per group). Scale bars represent 1 mm and 200  $\mu$ m (inset). **(f)** ASC<sup>+/+</sup> and ASC<sup>-/-</sup> cerebellar lysates at specified ages were immunoblotted as described above. **(g)** Immunohistochemistry (IHC) for phospho-histone H3 (pH3; Cell Signaling) in P7 ASC<sup>+/+</sup> and ASC<sup>-/-</sup> sagittal cerebellar sections. Quantitative comparison of cells expressing pH3 in ASC<sup>+/+</sup> and ASC<sup>-/-</sup> EGL ( $n=3-7$  per group). The EGL region was

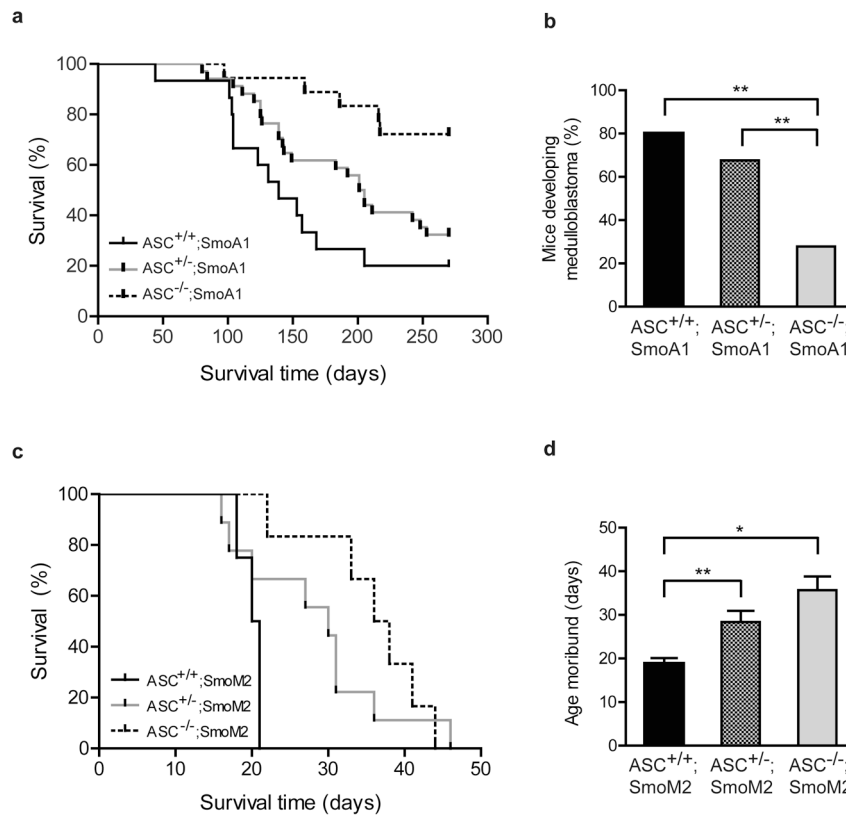
manually annotated using Aperio ImageScope V12 and analyzed with Aperio Nuclear V9 Algorithm (Aperio Technologies, Inc., Vista, CA, USA). The data represent mean  $\pm$  s.e.m. analyzed by Student's *t*-test. Scale bar represents 200  $\mu$ m.

Author Manuscript

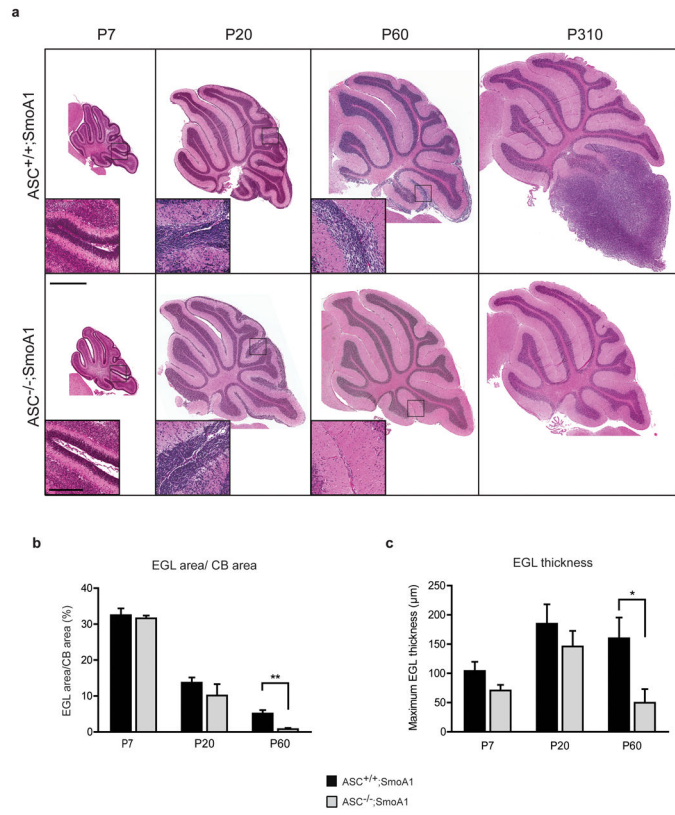
Author Manuscript

Author Manuscript

Author Manuscript



**Figure 2.** ASC deficiency suppresses medulloblastoma tumorigenesis in the SmoA1 and SmoM2 mouse models. **(a)** Kaplan-Meier analysis of ASC<sup>+/+</sup>;SmoA1 mice (n=15), ASC<sup>+/-</sup>;SmoA1 mice (n=34), and ASC<sup>-/-</sup>;SmoA1 mice (n=18) reveals a significant difference in tumor incidence with ASC expression ( $P=0.0019$ ; Log-Rank test). ASC deficiency significantly decreased tumor frequency and increased tumor latency when compared to ASC<sup>+/+</sup>;SmoA1 ( $P=0.0004$ ; Log-Rank test) and ASC<sup>+/-</sup>;SmoA1 mice ( $P=0.0077$ ; Log-Rank test). ( $P=0.1108$  between ASC<sup>+/-</sup>;SmoA1 and ASC<sup>+/+</sup>;SmoA1 mice; Log-Rank test.) **(b)** Overall incidence of medulloblastoma by P270 is reduced in ASC<sup>-/-</sup>;SmoA1 versus ASC<sup>+/+</sup>;SmoA1 ( $P=0.0049$ ; Fisher's exact test) and ASC<sup>+/-</sup>;SmoA1 ( $P=0.0088$ ; Fisher's exact test) mice;  $**P<0.01$ . **(c)** Kaplan-Meier analysis of ASC<sup>+/+</sup>;SmoM2 mice (n=4), ASC<sup>+/-</sup>;SmoM2 mice (n=9), and ASC<sup>-/-</sup>;SmoM2 mice (n=6) reveals a significant difference in tumorigenesis with ASC expression ( $P=0.0004$ ; Log-Rank test). ASC<sup>+/+</sup>;SmoM2 mice displayed shorter tumor latency than either ASC<sup>-/-</sup>;SmoM2 ( $P=0.0025$ ; Log-Rank test) or ASC<sup>+/-</sup>;SmoM2 ( $P=0.0003$ ; Log-Rank test) mice. ( $P=0.732$  between ASC<sup>+/-</sup>;SmoM2 and ASC<sup>-/-</sup>;SmoM2 mice; Log-Rank test.) **(d)** The average age mice become moribund is increased with ASC deficiency in ASC<sup>-/-</sup>;SmoM2 mice and ASC<sup>+/-</sup>;SmoM2 mice.  $**P=0.004$ ;  $*P=0.025$  (Student's *t*-test).



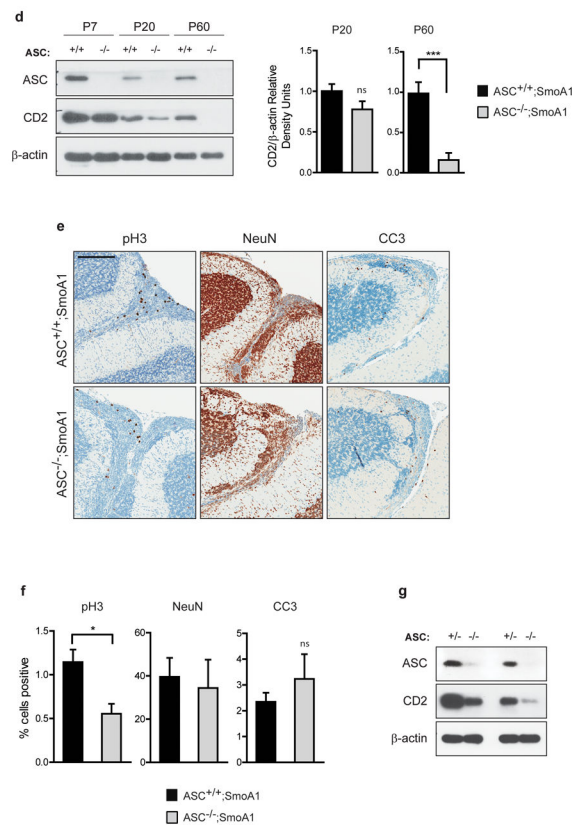


**Figure 3.**

ASC deficiency reduces proliferation in the SmoA1 cerebella *in vivo* and in *Smo* transgenic CGNPs *in vitro*. **(a)** Representative H&E stained sagittal sections of ASC<sup>+/+</sup>;SmoA1 and ASC<sup>-/-</sup>;SmoA1 cerebella at specified ages reveals reduced EGL with ASC deficiency. Scale bars represent 1 mm and 200  $\mu$ m (inset). **(b)** EGL area in proportion to cerebellum (CB) area and **(c)** maximum EGL thickness were manually quantified using Aperio ImageScope V12 annotations (Aperio Technologies, Inc.) in ASC<sup>+/+</sup>;SmoA1 and ASC<sup>-/-</sup>;SmoA1 cerebella at the specified ages (n=3–7 per group). ASC deficiency reduced EGL area proportion and maximum EGL thickness in P60 cerebella. \*\* $P=0.0049$ ; \* $P=0.045$  (Student's *t*-test). ASC status significantly altered both EGL proportion and thickness over all timepoints ( $P=0.035$  and  $P=0.04$  respectively; two-way ANOVA). **(d)** Western blot analysis of ASC<sup>+/+</sup>;SmoA1 and ASC<sup>-/-</sup>;SmoA1 cerebellar lysates at the specified ages as described above. Densitometric quantification reveals Cyclin D2 (CD2) levels are reduced at P20 ( $P=0.12$ ) and P60 (\*\* $P=0.00039$ ) with ASC deficiency. Data are mean  $\pm$  s.e.m. analyzed by Student's *t*-test (n=5–7 per group). **(e)** Representative IHC for pH3, NeuN (Millipore, Billerica, MA, USA), and cleaved caspase-3 (CC3; Biocare Medical, Concord, CA, USA) of P20 ASC<sup>+/+</sup>;SmoA1 and ASC<sup>-/-</sup>;SmoA1 cerebella. Scale bar represents 200  $\mu$ m. **(f)** Quantification of positively stained cells in the P20 EGL reveals a significant decrease in pH3 staining with ASC deficiency. \* $P=0.017$ . The data represent mean  $\pm$  s.e.m. analyzed by Student's *t*-test (n=3–5 per group). Quantification was performed as described in Figure 1f. **(g)** Western blot analysis shows a reduction in cyclin D2 levels with ASC deficiency in isolated SmoA1 cerebellar granule precursor cells. CGNPs were isolated from



ASC<sup>+/-</sup>;SmoA1 and ASC<sup>-/-</sup>;SmoA1 mice similarly to previously described<sup>46</sup>, with cells cultured for 48 hours in serum-free conditions. Results shown are from two independent sets of ASC<sup>+/-</sup>;SmoA1 and ASC<sup>-/-</sup>;SmoA1 mice.

Author Manuscript

Author Manuscript

Author Manuscript

Author Manuscript

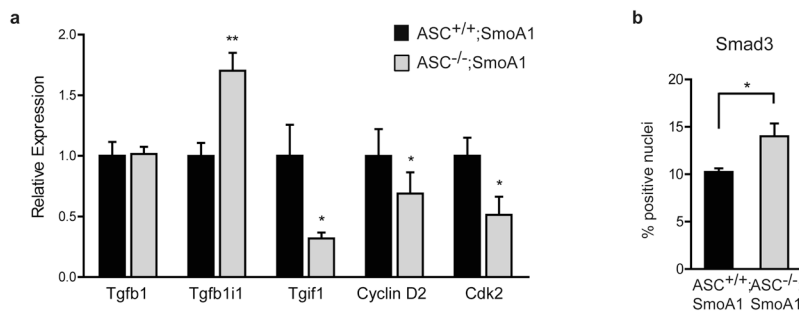


**Figure 4.**

ASC deficiency alters the TGF- $\beta$  pathway in SmoA1 cerebella. **(a)** Quantitative RT-PCR analysis reveals several genes in the TGF- $\beta$  pathway are differentially expressed in ASC<sup>-/-</sup> versus ASC<sup>+/+</sup> P20 SmoA1 cerebella. qRT-PCR was conducted similarly as previously described<sup>45</sup>, using primers *Tgfb1*-FW: 5'-ACCATGCCAACTTCTGTCTG-3' and *Tgfb1*-Rev: 5'-CGGGTTGTGTTGGTTGTAGA-3'; *Tgfb1i1*-FW: 5'-CCTTTTCGCCCCGAGTGCTA-3' and *Tgfb1i1*-Rev: 5'-CGGATGGGTTGGTTACAGAAG-3'; *Tgif1*-FW: 5'-GAGGATGAAGACAGCATGGA-3' and *Tgif1*-Rev: 5'-TTCTCAGCATGTCAGGAAG-3'; *Cyclin D2*-FW: 5'-TCGATGATTGCAACTGGAAG-3' and *Cyclin D2*-Rev: 5'-AGAGCTTCGATTGCTCCT-3'; *Cdk2*-FW: 5'-TCATGGATGCCTCTGCTCTCAC-3' and *Cdk2*-Rev: 5'-TGAAGGACACGGTGAGAATGGC-3'; *Gapdh*-FW: 5'-TGTGTCCGTCGTGGATCTGA-3' and *Gapdh*-Rev: 5'-CCTGCTTACCACCTTCTTGA-3', and normalizing to GAPDH levels. Data are mean  $\pm$  s.e.m analyzed by the Mann-Whitney test. Experiments were done in triplicate three to five times per gene (n=3–5 per genotype). \*\* $P$ <0.01; \* $P$ <0.05. **(b)** Quantification of Smad3 IHC (Abcam, Cambridge, MA, USA) in P20 ASC<sup>+/+</sup>;SmoA1 and ASC<sup>-/-</sup>;SmoA1 cerebella reveals an increase in cells positive for nuclear Smad3 with ASC deletion. 50  $\mu$ m wide bands of the outer internal granule layer and the molecular layer were manually annotated using Aperio ImageScope V12 and analyzed with Aperio Nuclear V9 Algorithm (Aperio Technologies, Inc.), excluding Purkinje cells from analysis using cell size parameters. \* $P$ <0.05. The data represent mean  $\pm$  s.e.m. analyzed by Student's  $t$ -test (n=3 per group).

**Table 1**  
**Summary of ASC expression in human medulloblastomas**

RNA *in situ* hybridization (ISH) of human medulloblastoma TMA sections was conducted for ASC with the RNAscope 2.0 HD Reagent Kit (BROWN) (Advanced Cell Diagnostics, Inc., Hayward, CA, USA) according to the manufacturer's instructions. Each tumor was scored for ASC signal as 0 (no signal), 1 (rare signal), 2 (scattered signal) or 3 (ubiquitous signal), with scores of at least 1.5 defined as positive for ASC expression. Samples were scored independently by two blinded observers, including one neuropathologist (RM), and any discrepant interpretations were resolved by consensus review. The formalin-fixed paraffin-embedded human tumor block was obtained from UNC Hospitals with approval by the Internal Review Board.

	ASC Positive	ASC Negative	Total
<b>Classic</b>	5	6	11
<b>Desmoplastic</b>	3	0	3
<b>Large cell/anaplastic</b>	1	0	1
<b>Overall (%)</b>	9 (60)	6 (40)	15 (100)

Author Manuscript

Author Manuscript

Author Manuscript

Author Manuscript

**Table 2**  
**Summary of genes differentially expressed with ASC deficiency in P20 SmoA1 cerebella**

Total RNA was purified from P20 SmoA1 cerebella (n=5, ASC<sup>+/+</sup>;SmoA1; n=4, ASC<sup>-/-</sup>; SmoA1) and 1000 ng RNA per sample was labeled using the Quick Amp Labeling Kit (Agilent Technologies, Sugar Land, TX, USA) and hybridized on two-color whole mouse genome 4×44K microarrays (Agilent Technologies). 1000 ng RNA from pooled P16 wild-type cerebella was amplified and labeled with Cy3 as a reference for each sample. Raw data was processed and analyzed by GeneSpring GX Version 11.0 (Agilent Technologies). Genes with a corrected *P* value <0.05 following unpaired *t*-test and Benjamini and Hochberg false discovery rate procedure were considered differentially expressed.

Symbol	RefSeq	Gene Name	Fold change	<i>P</i> value
<b>Up-regulated</b>				
<i>Gdpd3</i>	NM_024228	Glycerophosphodiester phospho-diesterase domain containing 3	+5.914	0.0268
<i>Tgfb1l1</i>	NM_009365	Transforming growth factor beta 1 induced transcript 1	+2.504	0.0494
<b>Down-regulated</b>				
<i>Sec23ip</i>	NM_001029982	Sec23-interacting protein	-1.492	0.0268